Inorg. Chem. **2003**, *42*, 8509–8518

Reactivity of $Ph_2P(Se)CH_2C_6H_4CH_2P(Se)Ph_2$ with $[M_3(CO)_{12}]$ (M = Ru or Fe). Synthesis and Characterization of the New Carbene Cluster $[Ru_3(\mu_3\text{-}Se)(\mu_3\text{-}H)(\mu_2\text{-}PPh_2)(CO)_6(\mu_2\text{-}CHC_6H_4CH_2PPh_2)]$

Daniele Belletti,[†] Claudia Graiff,*[,†] Chiara Massera,[†] Alex Minarelli,[†] Giovanni Predieri,[†] Antonio Tiripicchio,[†] and Domenico Acquotti[‡]

Dipartimento di Chimica Generale ed Inorganica, Chimica Analitica, Chimica Fisica, Università di Parma, Parco Area delle Scienze 17/A, and Centro Interdipartimentale Misure "Giuseppe Casnati", Università di Parma, Parco Area delle Scienze 23/A, 43100 Parma, Italy

Received July 27, 2003

The reactions of $[M_3(CO)_{12}]$ (M = Ru or Fe) with 1,2 bis[(diphenylphosphino)methyl]benzene diselenide ($dpmbSe_2$) in hot toluene afford a variety of phosphine-substituted selenido carbonyl clusters. They belong to the following three families: (i) 50-electron clusters with a M_3Se_2 core (**2**, **3**, **5**–**7**), (ii) 48-electron clusters with a M_3Se core (**1**, **8**), (iii) 34-electron clusters with a M_2Se_2 core (**4**). All these species derive from the P═Se bond cleavage. Cluster **1**, which contains a hydrido, a phosphido, and a carbene ligand, is produced by multiple fragmentation of the diphosphine. This fragmentation appears related to the presence of the selenido ligand on the cluster, as the reaction of $[Ru_3(CO)_{12}]$ with dpmb (not selenized) produces only carbonyl substitution by the phosphine to give $[Ru_3(CO)_{10}(\mu\text{-dpmb})]$ (**9**). All the clusters synthesized have been characterized by spectroscopic techniques, and in some cases fluxional behavior has been detected in solution by NMR analysis. The structures of **1**, **2**, and **7**–**9** have been determined by X-ray diffraction methods.

1. Introduction

The chemistry of transition-metal chalcogenido mono- and polynuclear complexes is a rapidly expanding research area, as pointed out in recent reviews.[1,2] The reasons for this increasing interest derive from the usefulness of these chalcogenido ligands in cluster growth reactions[3a] and from the search for precursors of extended inorganic solids with novel electronic, magnetic, and optical properties[3b] and for structural models.

In recent years we have carried out systematic investigations on the selenium transfer reactions by tertiary phosphine and diphosphine selenides, such as Ph_3PSe, $CH_2(Ph_2PSe)_2$ ($dppmSe_2$), $(CH_2Ph_2PSe)_2$ ($dppeSe_2$), and $Fe(\eta^5\text{-}C_5H_4Ph_2\text{-}PSe)_2$ ($dppfcSe_2$), toward iron and ruthenium carbonyl clusters.[4] These reactions take advantage of the frailty of the P═Se bond and provide a simple, sometimes selective,[5] synthetic route to phosphine-substituted, mono- and diselenido trinuclear clusters. Recently we have proved[6] that these reactions could proceed through two consecutive stepwise selenium transfers, leading first to the tetrahedral monoselenido $Ru_3(\mu_3\text{-}Se)$ and then to the square-pyramidal diselenido $Ru_3(\mu_3\text{-}Se)_2$ core clusters. Further pyrolytic processes usually lead to the formation of tetrahedral species M_2Se_2, in the case of iron, and octahedral species M_4Se_2, in the case of ruthenium (see Scheme 1). Occasionally, other less common compounds can be obtained via condensation processes such as clusters containing Ru_6Se_4 cores[7a] and the cubane-like cage complex with a Ru_4Se_4 core.[7b]

* Author to whom correspondence should be addressed. E-mail: claudia.graiff@unipr.it.

† Dipartimento di Chimica Generale ed Inorganica, Chimica Analitica, Chimica Fisica.

‡ Centro Interdipartimentale Misure.

(1) Roof, L. C.; Kolis, J. W. *Chem. Rev.* **1993**, *93*, 1037.

(2) Schmid, G., Ed. *Cluster and Colloids*; VCH: Weinheim, Germany, 1994; Chapter 3.

(3) (a) Dehnen, S.; Eichhofer, A.; Fenske, D. *Eur. J. Inorg. Chem*. **2002**, *2*, 279. (b) Steigerwald, M. L. *Polyhedron* **1994**, *13*, 1245.

(4) (a) Cauzzi, D.; Graiff, C.; Predieri, G.; Tiripicchio, A. In *Metal Cluster in Chemistry*; Braunstein, P., Oro, L., Raithby, P., Eds.; VCH: Weinheim, Germany, 1999; Vol. 1, p 193. (b) Graiff, C.; Predieri, G.; Tiripicchio, A. *Eur. J. Inorg. Chem*. **2003**, *9*, 1659.

(5) (a) Baistrocchi, P.; Cauzzi, D.; Lanfranchi, M.; Predieri, G.; Tiripicchio, A.; Tiripicchio Camellini, M. *Inorg. Chim. Acta* **1995**, *235*, 173. (b) Baistrocchi, P.; Careri, M.; Cauzzi, D.; Graiff, C.; Lanfranchi, M.; Manini, P.; Predieri, G.; Tiripicchio, A. *Inorg. Chim. Acta* **1996**, *252*, 367.

(6) Belletti, D.; Cauzzi, D.; Graiff, C.; Minarelli, A.; Pattacini, R.; Predieri, G.; Tiripicchio, A. *J. Chem. Soc., Dalton Trans.* **2002**, 3160.

10.1021/ic034887m CCC: $25.00
Published on Web 11/08/2003

Scheme 1

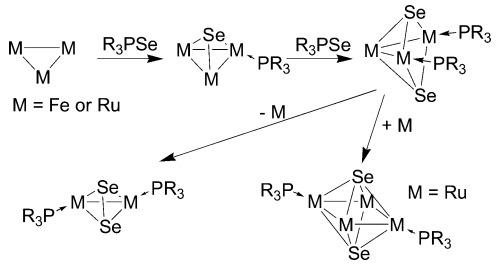

Recently we have also reacted different phosphine selenides with the tetrahedral clusters $[HMCo_3(CO)_{12}]$ (M = Fe or Ru) to obtain new chalcogenido carbonyl bimetallic clusters.[8] Mixed-metal clusters have been intensively studied in the last two decades, largely because of their often unique reactivity and catalytic properties and their role as molecular precursors to metal particles and novel heterogeneous catalysts.[9,10] Thus, the presence of different metals, which provide a larger diversity of possible coordination sites, can influence the selectivity of certain processes[11] and lead to the formation of compounds presenting new and not always easily predictable structures.

Continuing our investigations, we have also observed that tertiary phosphine selenides bearing heterocyclic fragments, such as 2-thienyl (th), 2-pyridyl (py), and 5-(2-pyridyl)-2-thienyl (pyth), can undergo multiple fragmentation by reaction with iron and ruthenium carbonyl clusters. In fact in the case of Ph_2(th)PSe and Ph_2(pyth)PSe with ruthenium, the reaction is not only limited to the transfer of the chalcogenido atom, but proceeds with P−C bond cleavage; new selenido phosphido clusters of formula $[Ru_3(\mu_3\text{-Se})(\mu\text{-}PPh_2)(\mu\text{-R})(CO)_6\{P(R)Ph_2\}]$ (R = th, pyth)[12,13] are obtained, whose molecular structures show the contemporary presence of the diphenylphosphido (bridging one side) and selenido (capping) ligands on the same cluster core. The reaction of Ph_2(py)PSe with $[Ru_3(CO)_{12}]$ results in the formation of the unprecedented compound $[Ru_3(\mu_3\text{-Se})(\mu\text{-}PPh_2)_2(\mu\text{-}C_5H_4N)(\mu_3\text{-}C_5H_4N)(CO)_6]$[14a] whose peculiarity lies in the unusual coordination mode of one pyridyl moiety, derived by the multiple fragmentation of the parent phosphine.

This paper deals with the reactions between $[M_3(CO)_{12}]$ (M = Ru or Fe) and the 1,2-bis[(diphenylphosphino)methyl]-benzene diselenide ($dpmbSe_2$) carried out with the aim to investigate the use of $dpmbSe_2$ as an effective precursor for dpmb-substituted ruthenium and iron selenido carbonyl clusters together with the complexing properties of this ligand. The preparation of dpmb has already been known for some time;[15] nevertheless, its coordination chemistry appears to have been little investigated.[16,17] In particular it has been utilized as a ligand in the synthesis of Pd,[18,19] Pt,[20−22] Ni,[22] and Ag[23] complexes, where the phosphine acts mostly as a chelating ligand, leading to the formation of stable seven-membered chelating rings, whose conformations have been studied in the solid state as well as in solution. Regarding the cluster chemistry, dpmb has never been used as a substituting ligand. Only recently sulfurated dpmb has been reacted with $[Ru_3(CO)_{12}]$, obtaining a class of sulfido carbonyl ruthenium clusters.[24]

2. Experimental Section

2.1. General Procedures. The starting reagents $[M_3(CO)_{12}]$ (M = Ru or Fe), $Ph_2PCH_2C_6H_4CH_2PPh_2$, and KSeCN were pure commercial products (Aldrich and Fluka) and were used as received. The solvents (C. Erba) were dried and distilled by standard techniques before use. All manipulations (prior to the TLC separations) were carried out under dry nitrogen by means of standard Schlenk-tube techniques. Elemental (C, H) analyses were performed with a Carlo Erba EA 1108 automated analyzer. IR spectra (KBr disks or CH_2Cl_2 solutions) were recorded on a Nicolet 5PC FT or a Nicolet Nexus FT spectrometer. Mass spectra were obtained using a Finnigan MAT SSQ710 spectrometer equipped with an EI/CI source, a direct inlet system, and a quadrupole mass analyzer. The CI source was utilized with methane as the reagent gas (*T* source, 220 °C; methane ionization energy, 70 eV). The quadrupole temperature was maintained at 140 °C; the system was scanned from 400 to 1600 amu, and negative ion (NICI) spectra were recorded.

2.2. Preparation and Reactions. 2.2.1. Preparation of $Ph_2P(Se)CH_2(C_6H_4)CH_2P(Se)Ph_2$, $dpmbSe_2$. The ligand $dpmbSe_2$ was prepared by selenium transfer from KSeCN. An excess of KSeCN (0.6 g, 4.2 mmol) was added to an acetonitrile solution (100 mL) of dpbm (0.5 g, 1.1 mmol), then the solution was stirred at room temperature for 2 h and dried in vacuo, and the residue was washed with water to remove the KCN formed. The rough product was then recrystallized from ethanol to obtain white crystals suitable for X-ray diffraction analysis. Yield: 0.6 g (90%). Anal. Found: C, 60.90; H, 4.40. Calcd for $C_{32}H_{28}P_2Se_2$: C, 60.95; H, 4.47. FTIR (KBr) (cm^{-1}): 525vs (ν(P═Se)). ^{1}H NMR ($CDCl_3$-d_1): δ 7.82−

(7) (a) Cauzzi, D.; Graiff, C.; Predieri, G.; Tiripicchio, A.; Vignali, C. *J. Chem. Soc., Dalton Trans.* **1999**, 237. (b) Cauzzi, D.; Graiff, C.; Lanfranchi, M.; Predieri, G.; Tiripicchio, A. *J. Chem. Soc., Dalton Trans.* **1995**, 321.
(8) Braunstein, P.; Graiff, C.; Massera, C.; Predieri, G.; Rosé, J.; Tiripicchio, A. *Inorg. Chem.* **2002**, *41*, 1372.
(9) Braunstein, P.; Rosé, J. Catalysis and Related Reactions with Compounds containing Heteronuclear Metal−Metal Bonds. In *Comprehensive Organometallic Chemistry II*; Abel, E. W., Stone, F. G. A., Wilkinson, G., Eds.; Pergamon Press: Oxford, 1995; Vol. 10, pp 351−385.
(10) Braunstein, P.; Rosé, J. Heterometallic Clusters in Catalysis. In *Metal Clusters in Chemistry*; Braunstein, P., Oro, L. A., Raithby, P. R., Eds.; VCH: Weinheim, Germany, 1999; Vol. 2, pp 616−677.
(11) Braunstein, P.; Sappa, E.; Tiripicchio, A. *Coord. Chem. Rev.* **1985**, *65*, 219.
(12) Cauzzi, D.; Graiff, C.; Massera, C.; Predieri, G.; Tiripicchio, A. *Inorg. Chim. Acta* **2000**, *300*−*302*, 471.
(13) Cauzzi, D.; Graiff, C.; Massera, C.; Predieri, G.; Tiripicchio, A. *J. Cluster Sci.* **2001**, *12*, 259.
(14) (a) Cauzzi, D.; Graiff, C.; Massera, C.; Predieri, G.; Tiripicchio, A. *Eur. J. Inorg. Chem.* **2001**, 721. (b) Fabrizi de Biani, F.; Graiff, C.; Opromolla, G.; Predieri, G.; Tiripicchio, A.; Zanello, P. *J. Organomet. Chem.* **2001**, *637*−*639*, 586.
(15) Aguiar, A. M.; Nair, M. G. R. *J. Org. Chem.* **1968**, *33*, 579.
(16) Rimmel, H. Dissertation, ETH Zürich, 1984; No. 7562.
(17) Rimml, H.; Venanzi, L. M. *Phosporus Sulfur* **1987**, *30*, 297.
(18) Werner, H.; Ebner, M.; Bertleff, W.; Schubert, U. *Organometallics* **1983**, *2*, 891.
(19) Paviglianiti, A. J.; Minn, D. J.; Fultz, W. C.; Burmeister, J. L. *Inorg. Chim. Acta* **1989**, *159*, 65.
(20) Ebner, M.; Otto, H.; Werner, H. *Angew. Chem., Int. Ed. Engl.* **1985**, *24*, 518.
(21) Werner, H.; Ebner, M.; Otto, H. *J. Organomet. Chem.* **1988**, *350*, 257.
(22) Camalli, M.; Caruso, F.; Chaloupka, S.; Leber, E. M.; Rimml, H.; Venanzi, L. M. *Helv. Chim. Acta* **1990**, *73*, 2263.
(23) Caruso, F.; Camalli, M.; Rimml, H.; Venanzi, L. M. *Inorg. Chem.* **1995**, *34*, 673.
(24) Belletti, D.; Graiff, C.; Lostao, V.; Pattacini, R.; Predieri, G.; Tiripicchio, A. *Inorg. Chim. Acta* **2003**, *347*, 137.

7.28 (m, 20H, Ph), 6.91 (m, 2H$_A$, H$_{ar}$), 6.56 (m, 2H$_B$, H$_{ar}$), 4.16 (d, $^2J_{HP}$ = 11 Hz, 4H, 2CH$_2$). ^{31}P NMR (CDCl$_3$-d_1): 29.7 (s, with ^{77}Se satellites, $^1J_{PSe}$ = 727 Hz).

2.2.2. Reaction of dpmbSe$_2$ with [Ru$_3$(CO)$_{12}$]. Synthesis of [Ru$_3$(μ_3-Se)(μ_3-H)(μ_2-PPh$_2$)(CO)$_6$(μ_2-CHC$_6$H$_4$CH$_2$PPh$_2$)] (1), [Ru$_3$(μ_3-Se)$_2$(CO)$_7$(dpmb)] (2), [Ru$_3$(μ_3-Se)$_2$(CO)$_7$(μ_2-dpmb)] (3), and [Ru$_2$(μ_2-Se$_2$)(CO)$_4$(μ_2-dpmb)] (4). Treatment of [Ru$_3$(CO)$_{12}$] (220 mg, 0.34 mmol) with 218 mg of dpmbSe$_2$ (0.34 mmol) and 28 mg of Me$_3$NO for 1.5 h in refluxing toluene, under N$_2$, gave a deep brown solution, which was evaporated to dryness, and the residue was redissolved in a small amount of dichloromethane. TLC separation on silica, using a CH$_2$Cl$_2$/petroleum ether (2:3) mixture as eluent, yielded a violet, a light orange, a dark orange, and a red band. The last three bands contained, respectively, the *nido* clusters **2** (yield 29%), **3** (yield 17%), and **4** (yield 23%). The structure of compound **2** was solved by X-ray diffraction, while those of compounds **3** and **4** were determined by comparison of spectroscopic data. The violet band afforded the cluster **1** (yield 19%), recognized after the solution of its crystal structure. Purification by crystallization (from a CH$_2$Cl$_2$/MeOH mixture at 5 °C for several days) gave well-formed crystals of **1** and **2** suitable for X-ray diffraction analysis.

Data for Cluster 1. IR (CH$_2$Cl$_2$, ν(CO), cm^{-1}): 2052w, 2031sh, 2015sh, 2007vs, 1965s. UV: λ (nm) 234 (λ_{max}) 272 (sh), 314 (sh), 573. $\epsilon \approx 4.8 \times 10^8$ L M^{-1} cm^{-1}. Anal. Found: C, 44.49; H, 2.80. Calcd for Ru$_3$SeP$_2$O$_6$C$_{38}$H$_{28}$: C, 44.59; H, 2.75. ^{31}P{^{1}H} NMR (CDCl$_3$-d_1): δ 40.1 (s, σ-PR$_3$), 247.0 (s, μ-PPh$_2$). ^{1}H NMR (CDCl$_3$-d_1): δ 10.14 (s, 1H$_c$), 7.75−7.20 (m, 20H, 4Ph), 7.67 (d, $^2J_{HAHB}$ = 7.8 Hz, 1H$_A$, H$_{ar}$), 7.24 (t, $^2J_{HAHB}$ = 7.8 Hz, $^2J_{HBHC}$ = 7.4 Hz, 1H$_B$, H$_{ar}$), 7.16 (t, $^2J_{HBHC}$ = 7.4 Hz, $^2J_{HCHD}$ = 7.4 Hz, 1H$_C$, H$_{ar}$), 7.06 (d, $^2J_{HCHD}$ = 7.4 Hz, 1H$_D$, H$_{ar}$), 3.53 (dd, $^2J_{HaHb}$ = 15 Hz, $^2J_{HaP}$ = 15 Hz, 1H$_a$, CH$_2$), 2.97 (dd, $^2J_{HbHa}$ = 15 Hz, $^2J_{HbP}$ = 9 Hz, 1H$_b$, CH$_2$), −14.58 (dd, $^2J_{HP}$ = 6 Hz, $^2J_{HP}$ = 15 Hz, 1H$_i$).

Data for Cluster 2. IR (CH$_2$Cl$_2$, ν(CO), cm^{-1}): 2066vs, 2033vs, 1991sh, 1986s, 1938w. MS-NICI: *m*/*z* (rel intens) 1103 (100), [Ru$_3$(μ_3-Se)$_2$(CO)$_6$(dpbm)]$^-$; 1075 (5), [Ru$_3$(μ_3-Se)$_2$(CO)$_5$(dpbm)]$^-$; 1047 (4), [Ru$_3$(μ_3-Se)$_2$(CO)$_4$(dpbm)]$^-$. Anal. Found: C, 41.47; H, 2.51. Calcd for Ru$_3$Se$_2$P$_2$O$_7$C$_{39}$H$_{28}$: C, 41.47; H, 2.49. ^{31}P{^{1}H} NMR (CD$_2$Cl$_2$): δ 40.8 (s, br). ^{1}H NMR (CDCl$_3$-d_1): δ 7.76−6.80 (m, 20H, 4Ph), 6.80 (m, 1H$_A$, H$_{ar}$), 6.41 (m, 1H$_B$, H$_{ar}$), 4.15 (dd, $^2J_{HaHb}$ = 13 Hz, $^2J_{HaP}$ = 9 Hz, 2H$_a$, CH$_2$), 3.80 (dd, $^2J_{HbHa}$ = 13 Hz, $^2J_{HbP}$ = 12 Hz, 2H$_b$, CH$_2$).

Data for Cluster 3. IR (CH$_2$Cl$_2$, ν(CO), cm^{-1}): 2061w, 2050vs, 2028w, 2015s, 1982m, 1944sh. MS-NICI: *m*/*z* (rel intens) 1131 (1), [Ru$_3$(μ_3-Se)$_2$(CO)$_7$(dpbm)]$^-$; 1103 (100), [Ru$_3$(μ_3-Se)$_2$(CO)$_6$(dpbm)]$^-$; 1075 (4), [Ru$_3$(μ_3-Se)$_2$(CO)$_5$(dpbm)]$^-$; 1047 (2), [Ru$_3$(μ_3-Se)$_2$(CO)$_4$(dpbm)]$^-$; 1019 (7), [Ru$_3$(μ_3-Se)$_2$(CO)$_3$(dpbm)]$^-$; 991 (12), [Ru$_3$(μ_3-Se)$_2$(CO)$_2$(dpbm)]$^-$; 1232 (2), [Ru$_4$(μ_3-Se)$_2$(CO)$_7$(dpbm)]$^-$. Anal. Found: C, 41.45; H, 2.47. Calcd for Ru$_3$Se$_2$P$_2$O$_7$C$_{39}$H$_{28}$: C, 41.47; H, 2.49. ^{31}P{^{1}H} NMR (CDCl$_3$-d_1): δ 43.7 (s), 46.8 (s). ^{1}H NMR (CDCl$_3$-d_1): δ 7.85−7.76 (m, 20H, 4Ph), 7.00 (m, 2H$_A$, H$_{ar}$), 6.86 (m, 2H$_B$, H$_{ar}$), 4.29 (m, 2H$_a$, CH$_2$), 3.32 (m, 2H$_b$, CH$_2$).

Data for Cluster 4. IR (CH$_2$Cl$_2$, ν(CO), cm^{-1}): 2055w, 2030s, 2001vs, 1985sh, 1958s, 1928sh. Anal. Found: C, 46.18; H, 2.95. Calcd for Ru$_2$Se$_2$P$_2$O$_4$C$_{36}$H$_{28}$: C, 45.77; H, 2.99. ^{31}P{^{1}H} NMR (CDCl$_3$-d_1): δ 38.2 (s, br). ^{1}H NMR (CDCl$_3$-d_1): δ 7.95−7.00 (m, 24H, 4Ph), 7.10 (m, 2H$_A$, H$_{ar}$), 6.86 (m, 2H$_B$, H$_{ar}$), 4.10 (m, 2H$_b$, CH$_2$), 3.75 (m, 2H$_a$, CH$_2$).

2.2.3. Reaction of dpmbSe$_2$ with [Fe$_3$(CO)$_{12}$]. Synthesis of [Fe$_3$(μ_3-Se)$_2$(CO)$_9$] (5), [{Fe$_3$(μ_3-Se)$_2$(CO)$_8$}$_2$(μ_2-dpmb)] (6), [Fe$_3$(μ_3-Se)$_2$(CO)$_7$(dpmb)] (7), and [Fe$_3$(μ_3-Se)(CO)$_8$(μ_2-dpmb)] (8). Treatment of [Fe$_3$(CO)$_{12}$] (170 mg, 0.34 mmol) with 214 mg of dpmbSe$_2$ (0.34 mmol) for 1.5 h in toluene at 70 °C, under N$_2$, gave a deep brown solution, which was evaporated to dryness, and the residue was redissolved in a small amount of dichloromethane. TLC separation on silica, using a petroleum ether/ethylic ether (2:1) mixture as eluent, yielded a bordeaux, a light brown, a black, and a brown band. The bordeaux and light brown bands contained, respectively, the *nido* clusters **5** (yield 25%) and **6** (yield 3%), identified by comparison of spectroscopic data.[25] The other two compounds were the *nido* clusters **7** (yield 31%) and **8** (yield 28%). Purification by crystallization (from a CH$_2$Cl$_2$/MeOH mixture at 5 °C for several days) gave well-formed crystals of **7** and **8** suitable for X-ray diffraction analysis.

Data for Cluster 5. IR (CH$_2$Cl$_2$, ν(CO), cm^{-1}): 2056vs, 2036s, 2013m, 1972sh. Anal. Found: C, 18.82. Calcd for Fe$_3$Se$_2$O$_9$C$_9$: C, 18.86.

Data for Cluster 6. IR (CH$_2$Cl$_2$, ν(CO), cm^{-1}): 2066m, 2053w, 2025s, 2002vs, 1977m, 1948w. Anal. Found: C, 36.82; H, 1.72. Calcd for Fe$_6$Se$_4$P$_2$O$_{16}$C$_{48}$H$_{28}$: C, 36.85; H, 1.80.

Data for Cluster 7. IR (CH$_2$Cl$_2$, ν(CO), cm^{-1}): 2051vs, 2013vs, 1982sh, 1977s, 1914w. MS-NICI: *m*/*z* (rel intens) 996 (8), [Fe$_3$(μ_3-Se)$_2$(CO)$_7$(dpbm)]$^-$; 968 (100), [Fe$_3$(μ_3-Se)$_2$(CO)$_6$(dpbm)]$^-$; 940 (10), [Fe$_3$(μ_3-Se)$_2$(CO)$_5$(dpbm)]$^-$; 586 (4), [Fe(CO)$_2$(dpbm)]$^-$. Anal. Found: C, 47.27; H, 2.86. Calcd for Fe$_3$Se$_2$P$_2$O$_7$C$_{39}$H$_{28}$: C, 47.24; H, 2.85. ^{31}P{^{1}H} NMR (CDCl$_3$-d_1, 298 K): δ 57.4 (s). ^{1}H NMR (CD$_2$Cl$_2$): δ 7.77−7.39 (m, 20H, 4Ph), 6.61 (dd, 2H$_A$, H$_{ar}$), 6.18 (dd, 2H$_B$, H$_{ar}$), 4.23 (dt, $^2J_{HaHb}$ = 13.4 Hz, $^2J_{HaP}$ = 2.5 Hz, 2H$_a$, CH$_2$), 3.58 (m, $^2J_{HbHa}$ = 13.4 Hz, $^2J_{HbP}$ = 6.8 Hz, 2H$_b$, CH$_2$).

Data for Cluster 8. IR (CH$_2$Cl$_2$, ν(CO), cm^{-1}): 2056w, 2043vs, 1988vs, 1864sh, 1783m. MS-NICI: *m*/*z* (rel intens) 945 (22), [Fe$_3$(μ_3-Se)(CO)$_8$(dpbm)]$^-$; 917 (22), [Fe$_3$(μ_3-Se)(CO)$_7$(dpbm)]$^-$; 889 (6), [Fe$_3$(μ_3-Se)(CO)$_6$(dpbm)]$^-$; 861 (9), [Fe$_3$(μ_3-Se)(CO)$_5$(dpbm)]$^-$; 833 (1), [Fe$_3$(μ_3-Se)(CO)$_4$(dpbm)]$^-$; 805 (1), [Fe$_3$(μ_3-Se)(CO)$_3$(dpbm)]$^-$; 777 (6), [Fe$_3$(μ_3-Se)(CO)$_2$(dpbm)]$^-$; 586 (100), [Fe(CO)$_2$(dpbm)]$^-$. Anal. Found: C, 51.02; H, 2.98. Calcd for Fe$_3$SeP$_2$O$_8$C$_{40}$H$_{28}$: C, 51.02; H, 2.99. ^{31}P{^{1}H} NMR (CD$_2$Cl$_2$): δ 67.8 (s). ^{1}H NMR (CDCl$_3$): δ 7.93−7.38 (m, 20H, 4Ph), 6.57 (m, 2 H$_A$, H$_{ar}$), 5.32 (m, 2 H$_B$, H$_{ar}$), 4.40 (dd, $^2J_{HaHb}$ = 13 Hz, $^2J_{HaP}$ = 5 Hz, 2H$_a$, CH$_2$), 3.34 (t, $^2J_{HaHb}$ = 13 Hz, $^2J_{HbP}$ = 14 Hz, 2H$_b$, CH$_2$).

2.2.4. Reaction of dpmb with [Ru$_3$(CO)$_{12}$]. Synthesis of [Ru$_3$(CO)$_{10}$(μ_2-dpmb)] (9). Treatment of [Ru$_3$(CO)$_{12}$] (220 mg, 0.34 mmol) with 163 mg of dpmb (0.34 mmol) and 26 mg of Me$_3$NO for 1.5 h in toluene at 90 °C, under N$_2$, gave a deep brown solution, which was evaporated to dryness, and the residue was redissolved in a small amount of dichloromethane. TLC separation on silica, using a CH$_2$Cl$_2$/petroleum ether (1:2) mixture as eluent, yielded a deep orange band together with a trace amount of another compound and decomposition. The separated band contained the trinuclear cluster **9** (yield 65%), which was identified by solving its crystal structure. Purification by crystallization (from a CH$_2$Cl$_2$/MeOH mixture at 5 °C for several days) gave well-formed crystals suitable for X-ray diffraction analysis. IR (CH$_2$Cl$_2$, ν(CO), cm^{-1}): 2095w, 2074s, 2063w, 2037m, 2004vs. Anal. Found: C, 47.39; H, 2.55. Calcd for Ru$_3$P$_2$O$_{10}$C$_{42}$H$_{28}$: C, 47.68; H, 2.65. MS-NICI: *m*/*z* (rel intens) 1057 (2), [Ru$_3$(CO)$_{10}$(dpbm)]$^-$; 973 (1), [Ru$_3$(CO)$_7$(dpbm)]$^-$; 945 (3), [Ru$_3$(CO)$_6$(dpbm)]$^-$; 917 (2), [Ru$_3$(CO)$_5$(dpbm)]$^-$; 889 (2), [Ru$_3$(CO)$_4$(dpbm)]$^-$; 861 (3), [Ru$_3$(CO)$_3$(dpbm)]$^-$; 833 (2), [Ru$_3$(CO)$_2$(dpbm)]$^-$; 805 (1), [Ru$_3$(CO)(dpbm)]$^-$; 777 (1), [Ru$_3$(dpbm)]$^-$;734 (100), [Ru$_2$(CO)$_2$(dpbm)]$^-$. ^{31}P{^{1}H} NMR (CDCl$_3$-d_1): δ 29.9 (s). ^{1}H NMR (CDCl$_3$-d_1): δ 7.47−7.32 (m, 20H, 4Ph),

(25) Cauzzi, D.; Graiff, C.; Lanfranchi, M.; Predieri, G.; Tiripicchio, A. *J. Organomet. Chem.* **1997**, *536*−*537*, 497.

Table 1. Proton NMR Chemical Shifts at 298 K for Compounds **1**−**4** and **7**−**9**

	H_a	H_b	H_c	H_i	H_A	H_B	H_C	H_D
1	3.53	2.97	10.14	−14.58	7.67	7.24	7.16	7.06
2	4.15	3.80			6.80	6.41		
3	4.29	3.32			7.00	6.86		
4	4.10	3.75			7.10	6.86		
7	4.23	3.58			6.61	6.18		
8	4.40	3.34			6.57	5.32		
9	3.84	3.84			6.67	5.83		

Table 2. Proton NMR Chemical Shifts at 198 K for the Two Conformations of Compound **2**

H_a	H_b	$H_{a'}$	$H_{b'}$	$H_{A'}$	$H_{B'}$	$H_{C'}$	$H_{D'}$
4.63	4.03	4.31	3.33	6.63	6.63	6.33	5.61
$H_{a''}$	$H_{b''}$	$H_{a'''}$	$H_{b'''}$	H_A	H_B	H_C	H_D
3.93	3.65	3.95	3.45	7.53	7.24	6.87	5.85

6.67 (m, $2H_A$, H_{ar}), 5.83 (m, $2H_B$, H_{ar}), 3.84 (d, $2H_{a,b}$ $^2J_{HP}$ = 11 Hz, 4H, CH_2).

2.3. NMR Data Collection and Structure Solution for Complexes 1−4 and 7−9. ^{1}H NMR spectra ($CDCl_3$ or CD_2Cl_2 solutions with TMS as internal reference) were recorded on AC300 and AMX400 Bruker instruments at 300 and 400 MHz, respectively, and ^{31}P NMR spectra at 81.0 MHz on a Bruker CXP 200 with 85% H_3PO_4 as external reference. Spectra were collected at different temperatures in the range 188−298 K. Complete assignments were obtained from the analyses of ^{1}H and ^{31}P 1D NMR spectra and of 2D COSY and NOESY spectra. Complete assignments for clusters **1**−**4** and **7**−**9** are listed in Tables 1 and 2.

2.4. X-ray Data Collection, Structure Solution, and Refinement for the dpmbSe$_2$ Ligand and the Complexes 1, 2, 7, 8·CH$_2$Cl$_2$, and 9·2H$_2$O. The intensity data were collected at room temperature on a Philips PW 1100 (compounds dpmbSe$_2$, **2**, **8**·CH_2Cl_2, and **9**·$2H_2O$) on a Siemens AED (compound **1**) single-crystal diffractometer and on a Bruker AXS Smart 1000 (compound **7**) single-crystal diffractometer equipped with an area detector using graphite-monochromated Mo Kα radiation. Crystallographic and experimental details for the structures are summarized in Table 3.

The structures were solved by Patterson and Fourier methods and refined by full-matrix least-squares procedures (based on F_o^2)[26] with anisotropic thermal parameters in the last cycles of refinement for all the non-hydrogen atoms except the carbon and chlorine atoms of the molecules of solvent in **8**·CH_2Cl_2. In the crystals of **8**·CH_2Cl_2 disordered molecules of CH_2Cl_2 were found distributed in two positions with occupancy factor 0.5, while in the crystals of **9**·$2H_2O$ water molecules were found. In all the structures the hydrogen atoms were introduced into the geometrically calculated positions and refined *riding* on the corresponding parent atoms, except those of the solvent molecules in **9**·$2H_2O$ and **8**·CH_2Cl_2 and except the hydride in **1**, which was localized in the ΔF map and refined isotropically. In the final cycles of refinement a weighting scheme, $w = 1/[\sigma^2F_o^2 + (0.0569P)^2 + 1.0764P]$ (dpmbSe$_2$), $w = 1/[\sigma^2F_o^2 + (0.0348P)^2]$ (**1**), $w = 1/[\sigma^2F_o^2 + (0.1000P)^2]$ (**2**), $w = 1/[\sigma^2F_o^2 + (0.0512P)^2]$ (**7**), $w = 1/[\sigma^2F_o^2 + (0.1735P)^2]$ (**8**·CH_2Cl_2), and $w = 1/[\sigma^2F_o^2 + (0.0571P)]$ (**9**·$2H_2O$), where $P = (F_o^2 + 2F_c^2)/3$, was used.

3. Results and Discussion

3.1 Syntheses and Spectroscopic Characterization. The selenuration of the diphosphine dpmb is based on selenium transfer from KSeCN at room temperature. The FTIR spectrum of dpmbSe$_2$ shows a band due to the P═Se stretching at 525 cm^{-1}. This absorption is quite strong and in good agreement with literature data.[27,28a] In the ^{31}P{^{1}H} spectrum a signal at δ 29.7 is present, the value of the chemical shift being higher compared with that of the starting phosphine (δ −13.5) owing to the deshielding effect of the selenium atom. The signal is a singlet with low-intensity satellites due to the coupling of ^{31}P with ^{77}Se (natural isotopic abundance 7.58%), the observed coupling constant $^1J_{PSe}$ being 727 Hz. In the ^{1}H spectrum the four methylenic protons give a doublet at δ 4.16, the multiplicity being due to the coupling with the two chemically equivalent phosphorus atoms ($^2J_{HP}$ = 11 Hz).

The transfer reactions of selenium atoms to the [$M_3(CO)_{12}$] cluster (M = Ru or Fe) by phosphine selenides generally suffer from scarce selectivity.[4] In the case of dpmbSe$_2$ the products obtained by this route (see Chart 1; carbonyls have been omitted for clarity) can be divided into three main families, the 50-electron clusters (7 skeletal electron pairs, sep's) with a M_3Se_2 core (**2**, **3**, **5**−**7**), the 48-electron clusters (6 sep's) with a M_3Se core (**1**, **8**), and the 34-electron cluster (6 sep's) with a M_2Se_2 core (**4**). Among the Ru_3Se family clusters, amounts of an unprecedented complex have been obtained (**1**). The phosphine selenide has suffered from multiple fragmentation, undergoing P═Se, P−C, and C−H bond cleavages.

Compound **1** is the result of a multiple addition of the fragments of the starting selenized ligand on the triangle metal cluster, leading to the formation of a hydride, a selenide, a phosphide, and a carbene ligand. Ruthenium carbene complexes have been widely used in the last years as models, precursors, and effective catalysts for olefin metathesis, ring-opening polymerization, and alkyne oligomerization.[29] This fact, along with the consideration that metal carbonyl clusters can represent a wide class of precursors and models for heterogeneous catalysis, results in a potential interest in compound **1**. The ^{31}P{^{1}H} NMR spectrum, recorded at room temperature, shows two sharp singlets at δ 40.1 and 247 due to the σ-coordinated phosphorus and to the phosphide group bridging one side of the metal triangle, respectively. The ^{1}H NMR spectrum, recorded from +11 to nearly −14 ppm, is reported in Figure 1. The complete proton assignment has been achieved by bidimensional NMR experiments (COSY, NOESY, TOCSY).

The μ_3-hydride H_i is found as a doublet of doublets at δ −14.58, due to the coupling with the two nonequivalent

(26) (a) *SMART Software Users Guide*, Version 5.1; Bruker Analytical X-ray Systems: Madison, WI, 1999. (b) *SAINT Software Users Guide*, Version 6.0; Bruker Analytical X-ray Systems: Madison, WI, 1999. (c) Sheldrick, G. M. *SADABS*; Bruker Analytical X-ray Systems: Madison, WI, 1999. (d) Sheldrick, G. M. *SHELXTL υ5.1: Program for the Refinement of Crystal Structures 97-2*; University of Göttingen: Göttingen, Germany, 1998.

(27) McFarlane, W.; Roycroft, D. S. *J. Chem. Soc., Dalton Trans.* **1973**, 2126.

(28) (a) Brown, D. H.; Cross, R. J.; Keat, R. *J. Chem. Soc., Dalton Trans.* **1980**, 871. (b) Ahrens, B.; Jones, P. G. *Acta Crystallogr., Sect. C: Cryst. Struct. Commun.* **1997**, *53*, 1852. (c) Hundal, R.; Lobana, T. S.; Turner, P. *Acta Crystallogr., Sect. E: Struct. Rep. Online* **2001**, *57*, 30. (d) Pilloni, G.; Longato, B.; Bandoli, G.; Corain, B. *J. Chem. Soc., Dalton Trans.* **1997**, 819.

(29) Adams, P. Q.; Davies, D. L.; Dyke, A. F.; Knox, S. A. R.; Mead, K. A.; Woodward, P. *Chem. Commun.* **1983**, 222.

Table 3. Crystal Data and Structure Refinement for Compounds $dpmbSe_2$, **1**, **2**, **7**, **8**·CH_2Cl_2, and **9**·$2H_2O$

	$dpmbSe_2$	**1**	**2**	**7**	**8**·CH_2Cl_2	**9**·$2H_2O$
empirical formula	$Se_2P_2C_{32}H_{28}$	$Ru_3SeP_2O_6C_{38}H_{28}$	$Ru_3Se_2P_2O_7C_{39}H_{28}$	$Fe_3Se_2P_2O_7C_{39}H_{28}$	$Fe_3SeP_2O_8C_{40}H_{28}$·CH_2Cl_2	$Ru_3P_2O_{10}C_{42}H_{28}$·$2H_2O$
fw	632.40	1024.71	1131.68	996.02	1030.00	1093.83
cryst syst	monoclinic	monoclinic	monoclinic	monoclinic	monoclinic	monoclinic
space group	*C*2/*c*	$P2_1/c$	$P2_1/c$	$P2_1/c$	$P2_1/n$	*C*2/*c*
unit cell dimensions (Å, deg)	$a = 23.451(5)$ $b = 9.226(5)$ $c = 26.289(5)$ $\beta = 98.120(5)$	$a = 15.212(4)$ $b = 12.963(3)$ $c = 18.904(5)$ $\beta = 100.53(3)$	$a = 11.400(4)$ $b = 19.107(5)$ $c = 18.973(3)$ $\beta = 102.16(3)$	$a = 11.451(4)$ $b = 18.732(5)$ $c = 18.798(5)$ $\beta = 102.53(5)$	$a = 18.357(4)$ $b = 14.313(3)$ $c = 16.731(5)$ $\beta = 90.71(3)$	$a = 46.185(5)$ $b = 9.993(5)$ $c = 22.311(3)$ $\beta = 118.26(2)$
V (Å^3)	5631(3)	3665(2)	4040(2)	3936(2)	4396(2)	9070(5)
Z, density(calcd) (Mg/m^3)	8, 1.492	4, 1.857	4, 1.861	4, 1.681	4, 1.556	8, 1.602
abs coeff (cm^{-1})	27.6	23.46	30.35	30.69	20.48	11.14
F(000)	2544	2000	2192	1976	2064	4336
cryst size (mm)	0.21 × 0.30 × 0.41	0.22 × 0.13 × 0.22	0.14 × 0.20 × 0.19	0.11 × 0.25 × 0.25	0.21 × 0.18 × 0.19	0.18 × 0.32 × 0.37
θ range (deg)	3.13−30.02	3.14−27.09	3.06−27.00	1.55−28.27	3.02−24.00	3.00−22.02
no. of reflns collected	8191	8322	8717	23231	7133	10688
no. of independent reflns	8191 [R(int) = 0.0]	8035 [$R_{int} = 0.0351$]	8408 [$R_{int} = 0.0657$]	8764 [$R_{int} = 0.0387$]	6884 [$R_{int} = 0.1447$]	5552 [$R_{int} = 0.0800$]
no. of obsd reflns [$I > 2\sigma(I)$]	4863	3745	3118	5462	3768	2673
no. of data/restraints/params	8191/0/329	8035/0/462	8408/0/485	8764/0/485	6884/6/517	5552/0/538
final R indices[a] [$I > 2\sigma(I)$]	R1 = 0.0458, wR2 = 0.1007	R1 = 0.0349, wR2 = 0.0697	R1 = 0.0336, wR2 = 0.0743	R1 = 0.0386, wR2 = 0.0830	R1 = 0.0906, wR2 = 0.3033	R1 = 0.0484, wR2 = 0.1192
R indices[a] (all data)	R1 = 0.1005, wR2 = 0.1220	R1 = 0.1019, wR2 = 0.0806	R1 = 0.1772, wR2 = 0.1529	R1 = 0.0836, wR2 = 0.0980	R1 = 0.1608, wR2 = 0.3432	R1 = 0.1255, wR2 = 0.1431

[a] $R1 = \sum||F_o| - |F_c||/\sum|F_o|$, $wR2 = [\sum[w(F_c^2 - F_o^2)^2]/\sum[w(F_o^2)^2]]^{1/2}$.

Chart 1

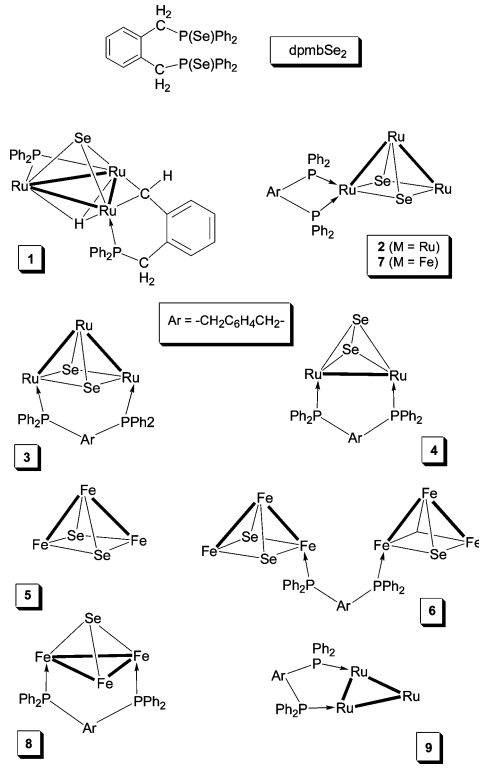

phosphorus atoms ($^2J_{HP} = 6$ and 15 Hz for the phosphide and the σ-coordinated phosphorus atom, respectively). The four aromatic protons H_A, H_B, H_C, and H_D give rise, as expected, to four different signals at δ 7.67, 7.24, 7.16, and 7.06, respectively; their complete assignment has been possible by studying both the 2D COSY and the 2D TOCSY spectra in the 7−8 ppm region. The two methylenic protons H_a and H_b are at δ 3.53 and 2.97, respectively ($^2J_{HaHb} = 15$ Hz); the multiplicity of the two signals is different due to their different values of the coupling constant with the phosphorus atoms. In fact, one of the hydrogen signals is a doublet of doublets with $^2J_{HbP} = 9$ Hz, while the other one

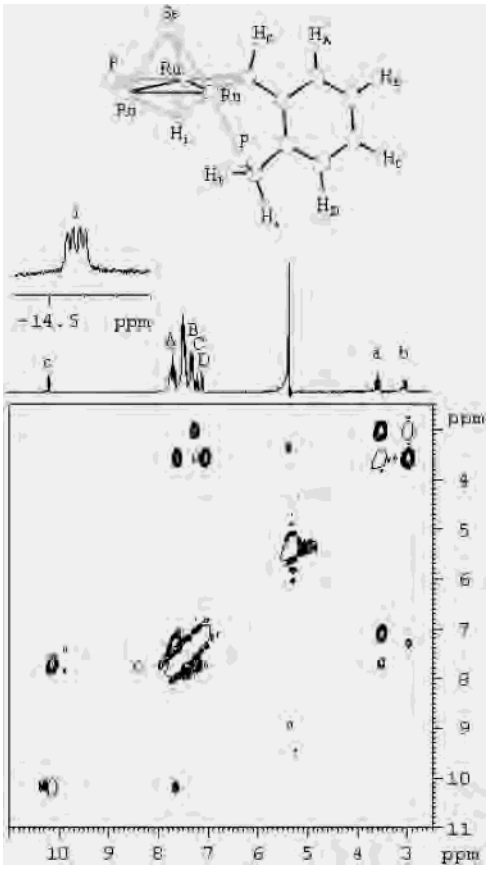

Figure 1. ^{1}H NOESY and ^{1}H NMR spectra (298 K) for compound **1**. The inset shows the resonance of the hydride ligand H_i. The NOESY positive cross-peaks are plotted at one level.

is a pseudotriplet with $^2J_{HaP} = {}^2J_{HaHb} = 15$ Hz. The carbene hydrogen gives a sharp singlet at δ 10.14. The 2D NOESY spectrum reveals the spatial proximity of H_c with H_A and H_i with H_b. It is also possible to see the correlation between the H_a proton and the H_D ring proton, which is at higher fields with respect to the other aromatic protons (see Figure 1). This well-defined conformation observed in solution is

the same as that adopted in the solid state where the separations H_c–H_A, H_i–H_b, and H_a–H_D are 2.227(7), 2.673(6), and 2.250(1) Å, respectively.

Compounds **2**, **3**, and **5**−**7** are 50-electron *nido* clusters which contain the well-known M_3Se_2 core (M = Ru or Fe). Those clusters are usually the most abundant products of this type of reaction.[4] Their core could be described as a squared base pyramid with two metal and two selenium atoms alternating at the base of the pyramid and the third metal atom at the apex of the pyramid. Cluster **5** has been recognized as $Fe_3Se_2(CO)_9$ by its well-known bordeaux color and by its IR spectrum in the carbonyl region.[4,25] Compound **6** is the substituted derivative where the phosphine ligand is bridging two cluster units through the P atoms.[4,25] In compounds **2** and **7** the phosphine chelates a basal metal atom, forming a seven-membered ring. The NICI mass spectra of **2** and **7** show the main peak corresponding to the fragment $[M_3(\mu_3\text{-}Se)_2(CO)_6(dpmb)]^-$ (M = Ru and Fe, *m*/*z* = 1103 and 968 for **2** and **7**, respectively) which derives from the cluster by loss of one carbonyl group. The other peaks correspond to the fragments $[M_3(\mu_3\text{-}Se)_2(CO)_5(dpmb)]^-$ (*m*/*z* 1075 (5) for M = Ru, *m*/*z* 940 (10) for M = Fe), and $[M_3(\mu_3\text{-}Se)_2(CO)_4(dpmb)]^-$ (*m*/*z* = 1047 (4) for M = Ru). In the case of the iron cluster it is possible to observe the molecular peak $[Fe_3(\mu_3\text{-}Se)_2(CO)_7(dpmb)]^-$ at *m*/*z* = 996 (22).

Structures of compounds **2** and **7** have been determined by NMR spectroscopy and X-ray diffraction methods. The phosphine chelates one of the ruthenium atoms at the base of the pyramid and shows fluxional behavior in solution. The ^{1}H NMR spectrum, recorded at room temperature, exhibits quite large signals, and the $^{31}P\{^1H\}$NMR spectrum of **2** reveals the presence of a large peak at δ 40.8. This suggests a fluxional behavior in solution which has been studied using multidimensional and variable-temperature NMR techniques. The two methylenic protons resonating at δ 3.80 and 4.15 give two doublets of doublets due to the different $^2J_{HH}$ and $^2J_{HP}$ values ($^2J_{HaHb}$ = 13 Hz, $^2J_{HbP}$ = 12 Hz, and $^2J_{HaP}$ = 9 Hz). The aromatic protons present two multiplets at δ 6.41 and 6.80. The peak at δ 6.80 has been assigned to hydrogen H_A by means of the 2D NOESY spectrum, being the only signal that does not give any correlation either with the geminal protons of the methylenic group or with the phenyl ring protons (see Figure 2a).

The ^{1}H and $^{31}P\{^1H\}$ NMR spectra recorded at 198 K show a more complicated pattern compared with those recorded at 298 K; in particular, the $^{31}P\{^1H\}$ spectrum shows two couples of doublets at δ 34.0 and 54.4 ($^2J_{PP}$ = 23 Hz) and at δ 40.1 and 53.2 ($^2J_{PP}$ = 28 Hz). This pattern suggests that cluster **2** in solution presents two different conformations with two nonequivalent phosphorus atoms; moreover, the difference in chemical shift (15−20 ppm) between the two doublet signals suggests that one of the phosphorus atoms is in an equatorial position, while the other one is in an axial position. This implies that in solution the cluster fluxionality mainly regards the phosphorus atoms, which exchange between the two different positions. The two conformations probably differ due to the presence of slow inversion processes on the phosphorus atoms or on the methylenic groups; in solution there is no evidence of a symmetrical structure as in the solid state. The nonequivalence of the phosphorus atoms influences the protons as well, since the ^{1}H NMR spectrum recorded at 223 K shows four different signals, both for the methylenic and the aromatic protons. At 198 K they become eight signals both for the methylenic and the aromatic protons, clearly indicating a number of different conformations for this cluster. The COSY spectrum (see Figure 3a) shows the correlations of two different patterns for aromatic protons (A, B, C, D and A′, B′, C′, D′) and four couples of signals for the methylenic protons (a, b; a′, b′; a″, b″; and a‴, b‴). The NOESY spectrum (see Figure 3b) allows the correlation of the A, B, C, D xylenic spin system with the a″, b″; a‴, b‴ methylenic protons and of the A′, B′, C′, D′ spin system with the a, b; a′, b′ protons. This suggests the presence of at least two different conformations completely assigned in Table 2.

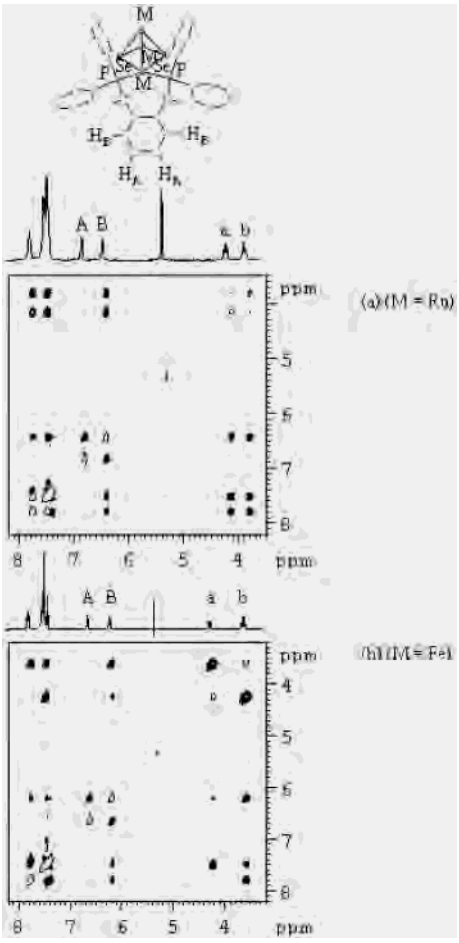

Figure 2. ^{1}H NOESY NMR spectra for compounds **2** (a) and **7** (b) (298 K). The NOESY positive cross-peaks are plotted at one level.

They are probably due to inversion processes on the carbon atoms. This could results in a *chair* and in a *boat* conformation of the seven-membered ring formed by Ru1, P1, C8, C9, C14, C15, and P2 atoms. Each methylenic and aromatic proton experiences different environments, showing different chemical shifts for both conformations.

Cluster **7** is isostructural with **2**. The $^{31}P\{^1H\}$ NMR spectrum recorded at room temperature shows a sharp singlet

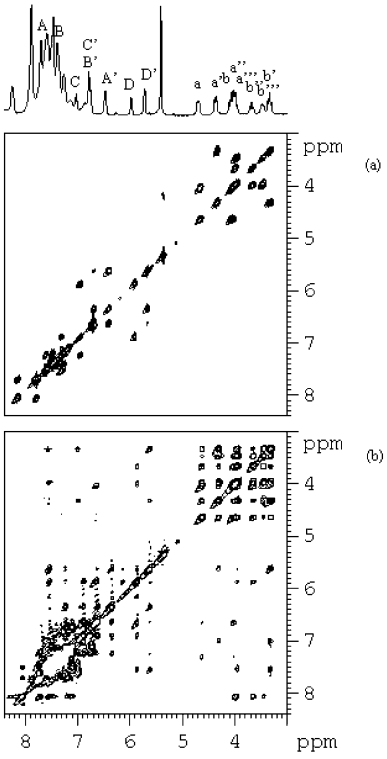

Figure 3. ^{1}H COSY (a), ^{1}H NOESY (b), and ^{1}H NMR spectra for compound **2** (198 K).

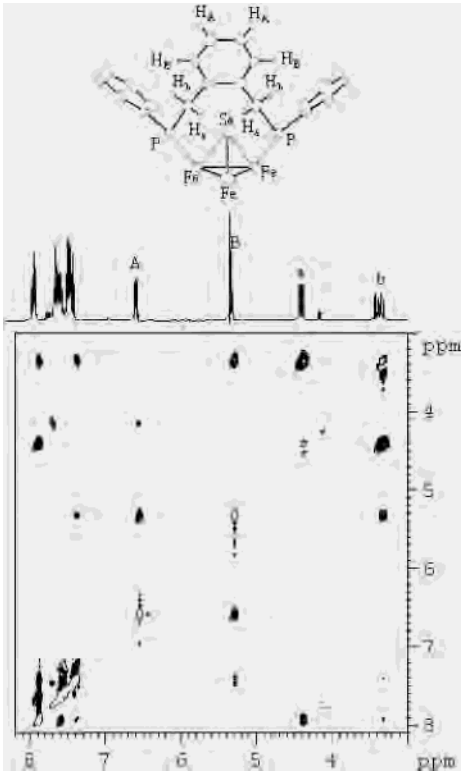

Figure 4. ^{1}H NOESY NMR spectrum for compound **8** (298 K). The NOESY positive cross-peaks are plotted at one level.

at δ 57.4; the ^{1}H NMR spectrum shows again three regions: the four methylenic protons give two signals at δ 3.58 and 4.23, the four xylenic protons give two signals at δ 6.18 and 6.61, and the phenyl groups resonate in the range 7.30−7.80 ppm. From the 2D NOESY spectrum the signal at δ 6.61 has been assigned to the H_A protons, since it does not show correlations either with the geminal methylenic protons or with the phenylic ones (see Figure 2b). Considering the methylenic protons, the signal at δ 4.23 appears as a doublet of triplets owing to the geminal coupling ($^2J_{HaHb}$ = 13.4 Hz) and to the virtual coupling with two phosphorus atoms (J_{HaP} = 2.5 Hz). Analogously the signal at δ 3.58 shows a $^2J_{HbHa}$ of 13.4 Hz and a J_{HbP} of 6.8 Hz.

Compound **3** is another 50-electron *nido* cluster, and it is an isomer of **2**, with the phosphine bridging the two ruthenium atoms at the base of the square pyramid; the NICI mass spectrum shows the molecular peak [Ru$_3$(μ_3-Se)$_2$(CO)$_7$-(μ-dpmb)]$^-$ at *m*/*z* 1131(1) (the main peak corresponds to the fragment [Ru$_3$(μ_3-Se)$_2$(CO)$_6$(μ-dpmb)]$^-$ which derives from the loss of one carbonyl ligand) and secondary peaks [Ru$_3$(μ_3-Se)$_2$(CO)$_n$(dpmb)]$^-$ (n = 2−7), due to the loss of other carbonyls.

Compound **8** is a 48-electron *nido* cluster with a Fe$_3$Se core in which the metal triangle is capped by a μ_3-selenium atom and the phosphine is bridging two of the iron atoms. The ^{31}P{^{1}H} NMR spectrum of this compound shows a singlet at δ 67.9, indicating that the two phosphorus atoms are chemically equivalent not only in the solid state but also in solution. The NICI mass spectrum shows that the fragmentation occurs for progressive loss of carbonyl groups, the fragments [Fe$_3$(μ_3-Se)(CO)$_n$(dpbm)]$^-$ (n = 2−8) being present. Compound **8** presents a pseudosymmetry plane which divides the molecule into two mirror halves; this symmetry is found in solution as well as in the solid state, as evidenced by the ^{31}P{^{1}H } and ^{1}H NMR spectra. The presence of sharp, well-defined peaks in a large temperature range (298−198 K) suggests that, if there is a fluxional behavior, it must be too fast to be detected on the NMR time scale. Neverthless, the presence of the bridging carbonyl group on the same Fe−Fe edge bridged by the phosphine could prevent any fluxional behavior similar to that described for **2** and **7**.

The ^{31}P{^{1}H } NMR spectrum shows a sharp singlet at δ 67.9 also at 198 K, thus providing further evidence for the equivalence of the two phosphorus atoms. The ^{1}H NMR spectrum shows the two methylenic hydrogen atoms H_a and H_b resonating at δ 4.40 and 3.34, respectively ($^2J_{HaHb}$ = 13 Hz). The signals present different multiplicities due to the different couplings of the protons with the phosphorus atoms: the δ 4.40 signal is a doublet of doublets ($^2J_{HaP}$ = 5 Hz), while the other one at δ 3.34 is a pseudotriplet with $^2J_{HbP}$ = 14 Hz. The four aromatic protons present two multiplets at δ 6.57 and 5.32, respectively. The latter indicates an unusual shift at high fields, which can be explained if proton H_b is under the shielding effect of the ring current of the adjacent phenyl groups. In fact, in the solid-state structure the average separation between H_B and the phenyl ring centroid is 2.88(1) Å. The 2D NOESY spectrum (see Figure 4) gives evidence for correlations between δ 3.34 and δ 5.32 peaks, allowing them to be assigned to H_b and H_B, respectively. In fact the solid structure confirmed this hypothesis, giving an average separation

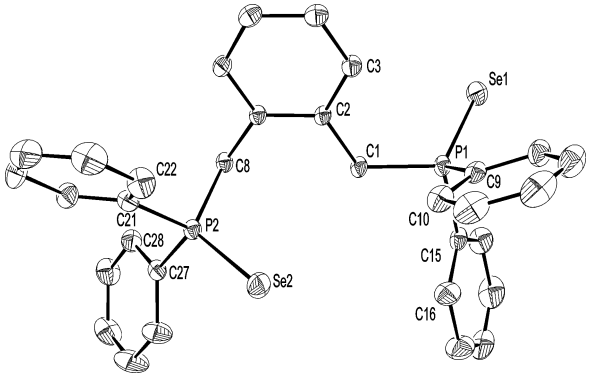

Figure 5. View of the molecular structure of $dpmbSe_2$ together with the atomic numbering system. Thermal ellipsoids are drawn at the 30% probability level.

between H_b and H_B of 2.502(1) Å. By lowering the temperature to 198 K, the 1D NMR spectrum pattern remains the same; only the δ 5.32 signal (H_B) is shifted 0.20 ppm to higher fields, probably because of the reinforcing of the ring current shielding.

Compound **4** is a 34-electron *nido* cluster with a Ru_2Se_2 core, in which the phosphine is bridging two bound ruthenium atoms. The identification has been obtained by comparing the FTIR spectrum of **4** in the carbonyl region with the FTIR spectrum of the iron cluster $[(Fe_2(\mu\text{-}Se_2)(CO)_4(\mu\text{-dppm})]$[25] and by the elemental analysis data.

To compare the reactivity toward clusters between $dpmbSe_2$ and its parent nonselenized phosphine (dpmb), we have also reacted dpmb with $[Ru_3(CO)_{12}]$, obtaining the substituted $[Ru_3(CO)_{10}(\mu\text{-dpmb})]$ cluster (**9**) as a unique major product. This result suggests that the P−C and C−H bond cleavages, which lead to the synthesis of **1**, in the case of $dpmbSe_2$, could be due to the presence of the chalcogen atom transferred to the ruthenium triangle, possibly inducing the P−C and C−H bond activations. This process is related to the behavior of the diphenylthienylphosphine selenide facing $[Ru_3(CO)_{12}]$.[12] In that case we observed that the presence of the capping selenido ligand on the metal triangle promoted the P−C(thienyl) cleavage not observed on the Ru_3 triangle without selenium. Compound **9** has been fully characterized by spectroscopic analysis and X-ray diffraction methods. The NICI mass spectrum shows the molecular peak $[Ru_3(CO)_{10}(\mu\text{-dpbm})]^-$ at *m*/*z* 1057 (2); the other peaks derive from the loss of other carbonyl groups. The $^{31}P\{^1H\}$ NMR spectrum of **9** shows a singlet at δ 29.9, indicating that the two phosphorus atoms are chemically equivalent not only in the solid state but also in solution. The ^1H NMR spectrum shows the four xylenic protons resonating as two multiplets at δ 6.67 and 5.83; also in this case the two H_B hydrogen atoms present a high-field shift, which can be explained with the shielding effect of the ring current of the adjacent phenyl groups, in analogy with what is observed in cluster **8**. In fact, in the solid-state structure the average distance between H_B and the phenyl ring centroid is 3.270(9) Å. Both the methylenic hydrogen atoms H_a and H_b resonate at δ 3.84 as a doublet ($^2J_{HP} = 11$ Hz). This can be explained considering a fast inversion of the methylenic groups, which equalizes the two nondiasterotopic hydrogen atoms.

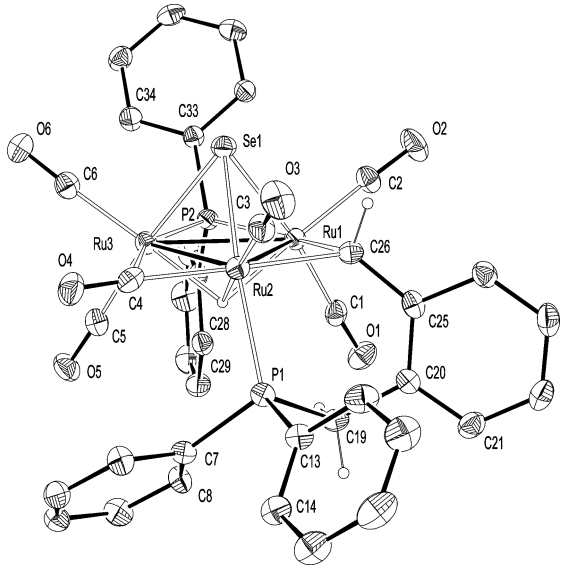

Figure 6. View of the molecular structure of **1** together with the atomic numbering system. Thermal ellipsoids are drawn at the 30% probability level.

Table 4. Selected Bond Distances (Å) and Angles (deg) for $dpmbSe_2$

P(1)−C(1)	1.823(3)	P(2)−C(8)	1.830(3)
P(1)−Se(1)	2.1157(9)	P(2)−Se(2)	2.1162(8)
C(7)−C(8)	1.519(4)	C(1)−C(2)	1.516(4)
C(9)−P(1)−Se(1)	113.98(11)	C(21)−P(2)−Se(2)	111.41(10)
C(1)−P(1)−Se(1)	114.01(10)	C(27)−P(2)−Se(2)	113.28(10)
C(15)−P(1)−Se(1)	113.16(12)	C(8)−P(2)−Se(2)	115.21(9)
C(2)−C(1)−P(1)	120.7(2)	C(7)−C(8)−P(2)	115.75(19)

Table 5. Selected Bond Distances (Å) and Angles (deg) for **1**

Ru(1)−C(26)	2.198(5)	Ru(2)−Ru(3)	2.8280(10)
Ru(1)−P(2)	2.3642(16)	Ru(3)−P(2)	2.2951(15)
Ru(1)−Se(1)	2.5290(9)	Ru(3)−Se(1)	2.5054(9)
Ru(1)−Ru(2)	2.7872(9)	P(1)−C(19)	1.822(5)
Ru(1)−Ru(3)	2.8443(8)	Ru(2)−Se(1)	2.5267(9)
Ru(2)−C(26)	2.150(5)	Ru(2)−P(1)	2.3192(15)
C(26)−Ru(1)−P(2)	160.12(13)	Ru(3)−Se(1)−Ru(1)	68.80(2)
Ru(2)−Ru(1)−Ru(3)	60.28(2)	Ru(2)−Se(1)−Ru(1)	66.91(3)
P(1)−Ru(2)−Se(1)	161.40(4)	C(19)−P(1)−Ru(2)	108.62(18)
Ru(1)−Ru(2)−Ru(3)	60.86(2)	Ru(3)−P(2)−Ru(1)	75.23(5)
Ru(2)−Ru(3)−Ru(1)	58.862(18)	C(25)−C(26)−Ru(2)	128.0(4)
Ru(3)−Se(1)−Ru(2)	68.39(3)	C(25)−C(26)−Ru(1)	121.7(3)

3.2. Crystal Structure Determination of $dpmbSe_2$, 1, 2, 7, 8·CH_2Cl_2, and 9·$2H_2O$. An ORTEP view of the molecular structure of $dpmbSe_2$ is given in Figure 5. A list of the selected bond distances and angles is given in Table 4. The P═Se bond distances are 2.1157(9) and 2.1162(8) Å.[28b−d]

The molecular structure of **1** is shown in Figure 6. A list of the selected bond distances and angles is given in Table 5. In compound **1** the triangular metal cluster is capped on one side by a μ_3-Se unit and on the other by a μ_3-H atom; it can be regarded as the result of a multiple addition, consisting in a selenium transfer accompanied by a P−C bond cleavage and by a hydride migration from the Ar−CH_2 group to the cluster. This fragmentation also produces a bridging carbene C26; this is the first reported crystal structure of a triangular ruthenium calchogenido complex containing a carbene moiety binding the Ru−Ru edge. In the CCDC data bank a

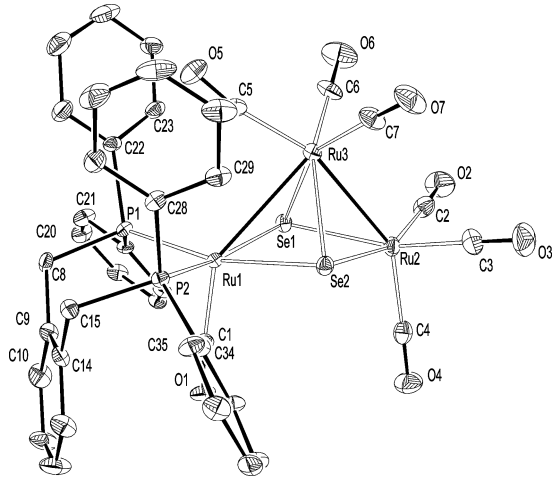

Figure 7. View of the molecular structure of **2** together with the atomic numbering system. Thermal ellipsoids are drawn at the 30% probability level.

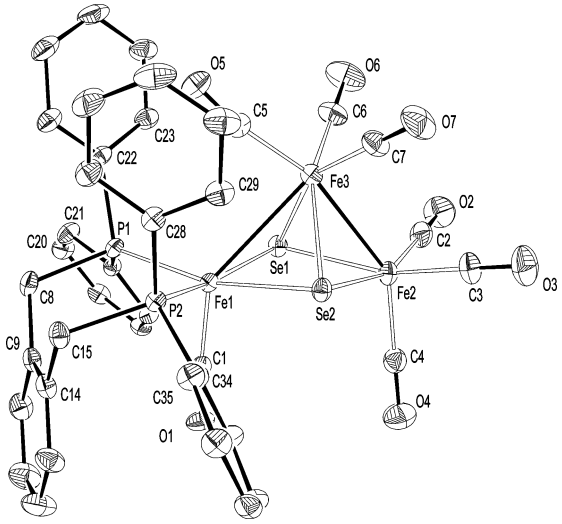

Figure 8. View of the molecular structure of **7** together with the atomic numbering system. Thermal ellipsoids are drawn at the 30% probability level.

dozen ruthenium compounds containing bridging μ_2 carbene moieties are present. The Ru−C bond distances span from 2.022 to 2.296 Å, and the Ru−C−Ru angles from 76.73° to 82.17°. In **1** the Ru1−C26 and Ru2−C26 bond distances are 2.198(5) and 2.150(5) Å, respectively, while the Ru1−C26−Ru2 bond angle is 79.72(3)°, in good agreement with what is reported above. The phosphorus atom P1 remains σ-coordinated on Ru2, while P2 bridges the Ru1−Ru3 edge as a phosphido ligand. The coordination around the metals is completed by six carbonyl groups, one of them asymmetrically bridging the Ru2−Ru3 edge (the bond distances Ru2−C4 and Ru3−C4 are 1.957(6) and 2.682(5) Å, respectively, and the Ru2−C4−O4 angle is 165.4(5)°). Even if all the Ru−Ru edges are bridged by different groups, the distances are only slightly different (Ru1−Ru2 = 2.787(1) Å, Ru2−Ru3 = 2.828(1) Å, Ru1−Ru3 = 2.844(1) Å). The three bridging atoms are slightly out of the metal triangle, P2 and C26 on the same side and opposite C4; C26 deviates 0.148(5) Å from the plane, while the selenium atom Se1 is displaced 1.924(1) Å from the same plane, a distance comparable with those found for the same class of compounds.[12−14] The bridging phosphine forms a six-membered ring through P1 and C26 of the carbene group; the ring shows a half-chair conformation [ΔC_2(C19−P1) = 0.247(2)].

ORTEP views of the molecular structures of isostructural clusters **2** and **7** are given in Figures 7 and 8, respectively. The lists of the selected bond distances and angles are given in Tables 6 and 7. These compounds are *nido* clusters with the well-known M_3Se_2 core, which can be described as a square pyramid with two metal and two selenium atoms alternating in the basal plane and the third metal atom at the apex of the pyramid.

The phosphine ligand chelates one of the metal atoms at the base of the pyramid, Ru1 or Fe1, the two phosphorus atoms substituting two carbonyl groups in equatorial positions. The bond distances Ru1−P1 and Ru1−P2 are equal, 2.350(3) and 2.349(3) Å, respectively, as are the Fe1−P1 and Fe1−P2 ones, 2.266(1) and 2.270(1) Å. The chelation

Table 6. Selected Bond Distances (Å) and Angles (deg) for **2**

Ru(1)−P(1)	2.350(3)	Ru(1)−P(2)	2.349(3)
Ru(2)−Se(1)	2.5055(15)	Ru(2)−Se(2)	2.5101(16)
Ru(1)−Se(1)	2.4785(14)	Ru(3)−Se(1)	2.5279(15)
Ru(1)−Se(2)	2.4977(14)	Ru(3)−Se(2)	2.5332(15)
Ru(1)−Ru(3)	2.9968(15)	Ru(2)−Ru(3)	2.7666(14)
P(1)−Ru(1)−P(2)	96.79(10)	Ru(1)−Se(1)−Ru(3)	73.53(4)
Se(1)−Ru(1)−Se(2)	80.37(4)	Ru(2)−Se(1)−Ru(3)	66.68(4)
Se(1)−Ru(2)−Se(2)	79.61(4)	Ru(1)−Se(2)−Ru(2)	98.84(5)
Se(1)−Ru(3)−Se(2)	78.76(5)	Ru(1)−Se(2)−Ru(3)	73.12(5)
Ru(2)−Ru(3)−Ru(1)	82.48(4)	Ru(2)−Se(2)−Ru(3)	66.54(4)
Ru(1)−Se(1)−Ru(2)	99.48(5)		

Table 7. Selected Bond Distances (Å) and Angles (deg) for **7**

Fe(1)−P(1)	2.2661(12)	Fe(1)−P(2)	2.2704(12)
Fe(2)−Se(1)	2.3758(9)	Fe(2)−Se(2)	2.3741(9)
Fe(1)−Se(1)	2.3371(8)	Fe(3)−Se(1)	2.3818(8)
Fe(1)−Se(2)	2.3593(9)	Fe(3)−Se(2)	2.3836(10)
Fe(1)−Fe(3)	2.8356(9)	Fe(2)−Fe(3)	2.6043(11)
P(1)−Fe(1)−P(2)	97.58(4)	Fe(1)−Se(1)−Fe(3)	73.86(2)
Se(1)−Fe(1)−Se(2)	80.78(2)	Fe(2)−Se(1)−Fe(3)	66.38(3)
Se(2)−Fe(2)−Se(1)	79.69(2)	Fe(1)−Se(2)−Fe(2)	98.49(2)
Se(1)−Fe(3)−Se(2)	79.37(3)	Fe(1)−Se(2)−Fe(3)	73.43(2)
Fe(2)−Fe(3)−Fe(1)	82.35(3)	Fe(2)−Se(2)−Fe(3)	66.38(2)
Fe(1)−Se(1)−Fe(2)	99.07(2)		

of the phosphine on Ru1 or Fe1 produces a lengthening of the side of the cluster:[4,30] the bond distance Ru1−Ru2 is 2.997(1) Å, while the Ru2−Ru3 bond distance is 2.767(1) Å (for compound **7**, Fe1−Fe2 = 2.836(2) Å, Fe2−Fe3 = 2.604(1) Å). The coordinated phosphine forms with M a seven-membered ring which presents a boat conformation, with the M, C9, and C14 atoms deviating in the same direction over the mean plane defined by P1, P2, C8, C15. The dihedral angles between the mean plane defined by P1, P2, C8, C15 and the xylene group are 69.0(2)° and 68.4(1)° (**2** and **7**, respectively).

In the crystals of **8** dichloromethane molecules of solvation are present. The structure of cluster **8** is shown in Figure 9. A list of the selected bond distances and angles is given in

(30) Cauzzi, D.; Graiff, C.; Massera, C.; Predieri, G.; Tiripicchio, A.; Acquotti, D. *J. Chem. Soc., Dalton Trans.* **1999**, 3515.

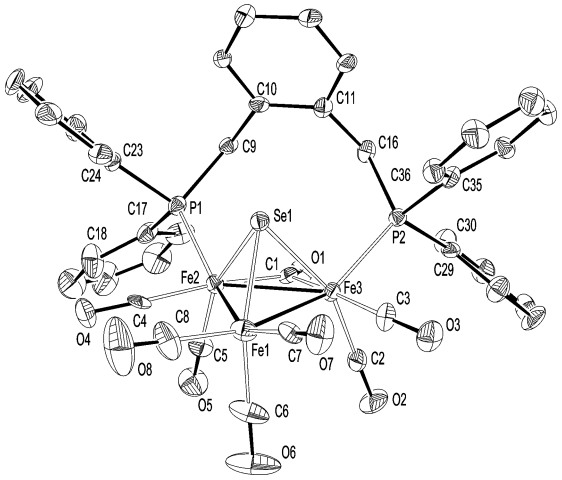

Figure 9. View of the molecular structure of **8** together with the atomic numbering system. Thermal ellipsoids are drawn at the 30% probability level.

Table 8. Selected Bond Distances (Å) and Angles (deg) for **8**

Fe(2)−Fe(3)	2.553(3)	Fe(1)−Se(1)	2.318(3)
Fe(1)−Fe(2)	2.590(3)	Fe(2)−Se(1)	2.362(2)
Fe(1)−Fe(3)	2.606(3)	Fe(3)−Se(1)	2.361(2)
Fe(2)−P(1)	2.221(4)	Fe(3)−P(2)	2.238(4)
Fe(2)−Fe(1)−Fe(3)	58.87(8)	Fe(1)−Se(1)−Fe(3)	67.69(8)
Fe(3)−Fe(2)−Fe(1)	60.90(8)	Fe(1)−Se(1)−Fe(2)	67.19(9)
Fe(2)−Fe(3)−Fe(1)	60.24(8)	Fe(3)−Se(1)−Fe(2)	65.44(8)
P(1)−Fe(2)−Fe(1)	145.28(14)	P(2)−Fe(3)−Fe(1)	147.48(14)

Table 8. The structure shows a metal triangle capped by a selenium atom, which is 1.881(1) Å from the plane passing through the iron atoms.

The bond distance Se1−Fe1 (2.318(3) Å) is shorter than the Se1−Fe2 (2.362(2) Å) and the Se1−Fe3 (2.361(2) Å) distances, probably because of the presence of the bulky xylene group which forces the selenium atom toward Fe1. The phosphine and a carbonyl group bridge the Fe2−Fe3 side (2.553(3) Å), which is shorter than the other Fe2−Fe1 (2.590(3) Å) and Fe3−Fe1 (2.606(3) Å) sides. The phosphine substitutes two carbonyl groups in pseudoaxial positions, the dihedral angle between the mean plane defined by P1, P2, Fe2, Fe3 and the metal triangle being 39.1(1)°. The phosphine forms with Fe2 and Fe3 an eight-membered ring which presents an envelope conformation, C10 and C11 deviating on the same side from the mean plane defined by Fe2, Fe3, P1, P2, C9, C16; the dihedral angle between this plane and the xylene group is 74.6(2)°.

The ORTEP view of the molecular structure of **9** is given in Figure 10. A list of the selected bond distances and angles is given in Table 9. The structure displays a triangular metal cluster, which derives from $[Ru_3(CO)_{12}]$ by substitution of two terminal carbonyl groups in pseudoequatorial positions by a molecule of the bidentate phosphine ligand. The dihedral angle between the mean plane defined by Ru1, Ru2, P1, P2 and the metal triangle is 3.7(1)°. The phosphine bridges the longest Ru−Ru edge of the metal triangle (Ru1−Ru2 = 2.943(2) Å). The Ru1−Ru3 and Ru3−Ru2 bond distances are 2.895(2) and 2.901(2) Å, respectively, in good agreement with those found in $[Ru_3(CO)_{12}]$.[31] The phosphine forms with Ru1 and Ru2 an eight-membered ring which presents an envelope conformation, C12 and C17 deviating on the same side over the mean plane defined by Ru1, Ru2, P1, P2, C11, C18; the dihedral angle between this plane and the xylene group is 88.9(2)°.

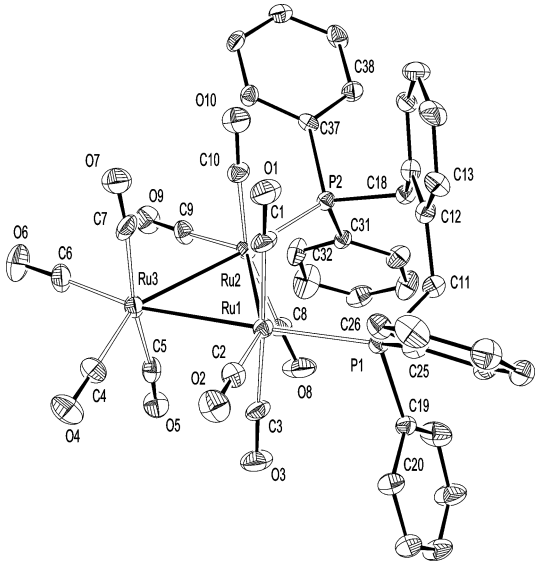

Figure 10. View of the molecular structure of **9** together with the atomic numbering system. Thermal ellipsoids are drawn at the 30% probability level.

Table 9. Selected Bond Distances (Å) and Angles (deg) for **9**

Ru(2)−Ru(3)	2.9009(15)	Ru(1)−P(1)	2.350(3)
Ru(1)−Ru(3)	2.8955(15)	Ru(2)−P(2)	2.349(3)
Ru(1)−Ru(2)	2.9431(16)		
P(1)−Ru(1)−Ru(3)	166.02(9)	P(2)−Ru(2)−Ru(3)	174.84(9)
P(1)−Ru(1)−Ru(2)	108.17(9)	P(2)−Ru(2)−Ru(1)	125.59(9)
Ru(3)−Ru(1)−Ru(2)	59.58(4)	Ru(3)−Ru(2)−Ru(1)	59.40(4)
Ru(1)−Ru(3)−Ru(2)	61.03(4)		

Acknowledgment. Financial support from the Ministero dell'Università e della Ricerca Scientifica e Tecnologica (Roma, Cofin 98) is gratefully acknowledged. The facilities of the Centro Interdipartimentale di Misure (Università di Parma) were used to record the NMR and mass spectra.

Supporting Information Available: Complete listings of atomic positions, bond lengths and angles, anisotropic thermal parameters, hydrogen atom coordinates, data collection, and crystal parameters for all crystallographically characterized complexes in CIF format. This material is available free of charge via the Internet at http://pubs.acs.org.

IC034887M

(31) (a) Churchill, T. R.; Hollander, F. J.; Hutchinson, J. P. *Inorg. Chem.* **1977**, *16*, 265. (b) Braga, D.; Grepioni, F.; Tedesco, E.; Dyson, R. J.; Martin, C. M.; Johnson, B. F. G. *Transition Met. Chem. (Dordrecht, Neth.)* **1995**, *20*, 615.